

Modulational instability and solitary waves in one-dimensional lattices with intensity-resonant nonlinearity

Milutin Stepić*

Vinča Institute of Nuclear Sciences, P. O. Box 522, 11001 Belgrade, Serbia

Aleksandra Maluckov and Marija Stojanović

Faculty of Mathematics and Sciences, University of Niš, P. O. Box 224, 18001 Niš, Serbia

Feng Chen

School of Physics, Shandong University, 250100 Jinan, China

Detlef Kip

Institute of Physics and Physical Technologies, Clausthal University of Technology, 38678 Clausthal-Zellerfeld, Germany

(Received 28 August 2008; published 17 October 2008)

We study theoretically light beam propagation in one-dimensional periodic media with intensity-resonant nonlinearity. The phenomenon of discrete modulational instability is investigated in detail as well as the conditions for the existence and stability of fundamental lattice and surface soliton modes. According to the linear stability analysis, only on-site solitons are stable. The mobility of lattice solitons is analyzed by both free energy and mapping concepts. Only broad solitons may freely traverse the lattice.

DOI: [10.1103/PhysRevA.78.043819](https://doi.org/10.1103/PhysRevA.78.043819)

PACS number(s): 42.65.Tg, 63.20.Pw, 42.25.Gy

I. INTRODUCTION

Discrete spatial solitons are robust nonlinear structures capable of maintaining their shape during propagation. In lossless media, they are conditioned by an exact balance between diffraction and nonlinearity. Such stable structures naturally emerge as convenient energy carriers in various settings including Bose-Einstein condensates [1], biomolecules [2], and nonlinear transmission lines [3]. Experimentally, research into discrete solitons in nonlinear optics has proved to be particularly successful and there are many research reports that witness in favor of the feasibility of an all-optical concept. Uniform nonlinear waveguide arrays (NWAs) represent an arrangement of mutually parallel channel waveguides that are weakly (linearly) coupled. Discrete solitons in NWAs were proposed two decades ago [4] and observed thereafter in media exhibiting cubic [5], saturable [6], quadratic [7], and nonlocal [8] nonlinear responses, to cite only a few.

There is an ongoing demand for reliable, low-cost, and environment-friendly optical materials with fast response at low power level [9]. Indium phosphide (InP) is a binary semiconductor with zinc-blende crystal structure and $F\bar{4}3m$ group symmetry. This material is extensively used in high-power and high-frequency electronics because of its superior electron mobility with respect to the more common semiconductors silicon and gallium arsenide. It possesses a direct band gap, making it useful for optoelectronic devices like laser diodes. Moreover, InP has one of the longest lifetimes of optical phonons of any compound with the zinc-blende crystal structure. This photorefractive semiconductor has a tiny electro-optic coefficient which, in turn, would require

high applied fields for external biasing. On the other hand, it has been shown that InP doped with iron (InP:Fe) exhibits a resonant enhancement of both light-induced space-charge fields and two-wave mixing gain with a measured microsecond response at microwatt power level and telecommunication wavelengths [10–12]. Self-deflection, self-focusing, and spatial solitons in this material have been investigated recently in the bulk [13–15].

In this paper, we present a theoretical model for light propagation in periodic media with intensity-resonant nonlinearity (Sec. II), briefly discuss the phenomenon of discrete modulational instability (Sec. III), and investigate the existence and stability of lattice and surface solitons (Sec. IV). One part of Sec. IV is devoted to soliton mobility. Finally, conclusions are given in Sec. V.

II. MATHEMATICAL MODEL

Paraxial optical beam propagation in linear one-dimensional (1D) periodic media may be described by the following partial differential equation [16]:

$$i \frac{k_z}{k} \frac{\partial U}{\partial z} + \frac{1}{2k} \frac{\partial^2 U}{\partial x^2} - \frac{k_z^2}{2k} U + \frac{kn_r(x)}{n_0} U = \beta U, \quad (1)$$

where x stands for the transverse coordinate, U is the amplitude of the electric field, β is the linear propagation constant, k_x denotes the transverse component (Bloch momentum) of wave number $k=2\pi n_0 \lambda_0^{-1}$, and λ_0 represents the (vacuum) wavelength of light. To a good extent, the periodically modulated refractive index, which defines the periodic lattice, may be described by $n_r(x)=n_0+\alpha \cos^2(\pi x/\Lambda)$ where n_0 is the refractive index of the light in the substrate ($n_0=3.205$ for InP:Fe at $\lambda_0=1.3159 \mu\text{m}$), α is the modulation amplitude, and Λ is the period of the lattice. This equation can be solved

*mstepic@vinca.rs

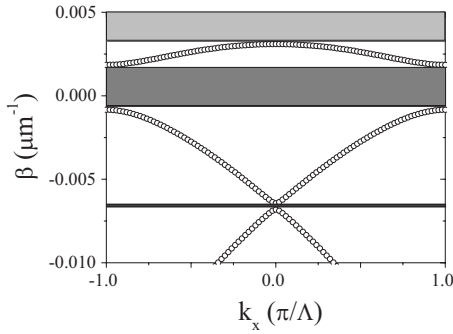


FIG. 1. Linear band gap structure of a NWA with lattice period of 12.6 μm .

analytically by the plane wave decomposition method [17]. As an example, in Fig. 1 is given the linear band gap structure of a 1D periodic structure in InP:Fe with lattice period of 12.6 μm . Here, only the first three bands together with the tiny second gap (dark gray), the first gap (gray), and the lowest part of the semi-infinite total internal reflection gap (light gray) are shown.

If light-induced refractive index changes are not negligible, a nonlinear contribution Δn should be included in the expression for $n_r(x)$ in Eq. (1). In photorefractives, $\Delta n = -0.5n_0^3 r E_{\text{sc}}$ where r denotes the corresponding electro-optic coefficient and E_{sc} stands for the space-charge field induced in the sample [18]. For InP $r \approx r_{41} = -1.42 \times 10^{-12}$ pm/V [12] while, according to Ref. [13],

$$E_{\text{sc}} = E_0 \frac{I_{r0} - I_d}{I_{r0} - I}, \quad (2)$$

where the applied electrical field is denoted by E_0 while I_d , I_{r0} , and I are the dark irradiance, resonant intensity, and intensity, respectively.

As demonstrated in Ref. [19], bright unstaggered lattice solitons can exist in regions where the effects of normal diffraction and self-focusing nonlinearity cancel each other. On the other hand, bright staggered localized modes may be found in gaps between allowed bands provided that a self-defocusing nonlinearity balances anomalous diffraction. Localized modes, whose propagation constants are pushed by nonlinear effects into the gaps of the linear structure, are also known as gap or Bragg solitons [20].

Nonlinear optical beam propagation within the first band of an arbitrary periodic structure may be fairly well described by a discrete model based on the coupled mode approach [4]. Thus, our intensity-resonant continuous model equations may be simplified by neglecting the dark irradiance and reduced [13,18,21] to the following set of nondimensional ordinary differential equations:

$$i \frac{dU_n}{d\xi} + U_{n+1} + U_{n-1} - 2U_n + \gamma \frac{U_n}{1 - |U_n|^2} = 0, \quad (3)$$

in which U_n is the normalized amplitude of the electrical field in the n th element of the lattice, $\xi = z/kx_0^2$ represents the normalized propagation coordinate, and γ is a normalized nonlinear coefficient, which can be either positive (in self-

focusing media, $E_0 > 0$) or negative (in self-defocusing media, $E_0 < 0$). Resonance occurs for $|U_n|^2 = 1$. There are only two integrals of motion: the power $P = \sum |U_n|^2$ and the Hamiltonian $H = \sum [|U_{n-1} - U_n|^2 + \gamma \ln(1 - |U_n|^2)]$; thus the system is not integrable in the general case.

III. MODULATIONAL INSTABILITY

The simplest solution of Eq. (3) is a plane wave (uniform) solution of the form $U_n = U_0 e^{iKn - i\omega\xi}$ with $K=0$ for the unstaggered case (adjacent elements are in phase) and $K=\pi$ for the staggered case (adjacent elements are out of phase). In this work we focus on the self-focusing case, while the effect of a defocusing nonlinearity will be investigated in detail elsewhere. Our plane wave amplitude reads $U_0 = \sqrt{(\omega + \gamma)/\omega}$ where $\omega \notin (-\gamma, 0]$. This solution becomes modulationally unstable, splitting eventually into a train of spatial solitons. The underlying effect of discrete modulational instability (MI) has been investigated in photonic lattices with both self-focusing [4,22] and self-defocusing nonlinearities [23,24].

By inserting a perturbed solution $[U_0 e^{iKn} + \delta U_n(\xi) e^{i\kappa n}] e^{-i\omega\xi}$ into Eq. (3), where $|\delta U_n| \ll U_0$, and $\kappa=0$ and $\kappa=\pi$ denote unstaggered and staggered perturbation, respectively, one can show that the following difference-differential equations for small perturbations are satisfied:

$$i \frac{d\delta U_n}{d\xi} + \cos \kappa (\delta U_{n+1} + \delta U_{n-1}) - 2\delta U_n + \gamma \frac{U_0^2}{(1 - |U_0|^2)^2} (\delta U_n + \delta U_n^*) = 0. \quad (4)$$

By adopting the complex perturbation form from Ref. [4], $\delta_n = \epsilon_1 \exp[i(Q\xi - n\Omega\Lambda)] + \epsilon_2 \exp[-i(Q\xi - n\Omega\Lambda)]$, in which $\epsilon_{1,2}$ are constants while Q and Ω are parameters of a modulated wave, we obtain the following dispersion relation:

$$Q^2 = 8 \sin^2\left(\frac{\Omega\Lambda}{2}\right) \left[2 \sin^2\left(\frac{\Omega\Lambda}{2}\right) - \gamma \frac{U_0^2}{(1 - |U_0|^2)^2} \right]. \quad (5)$$

Instability shows up provided that $Q^2 < 0$, which leads to the conclusion that the MI region is bounded from both below and above:

$$1 + \frac{\gamma}{4 \sin^2(\Omega\Lambda/2)} \left(1 - \sqrt{1 + \frac{4 \sin^2(\Omega\Lambda/2)}{\gamma}} \right) < U_0^2 < 1 + \frac{\gamma}{4 \sin^2(\Omega\Lambda/2)} \left(1 + \sqrt{1 + \frac{4 \sin^2(\Omega\Lambda/2)}{\gamma}} \right). \quad (6)$$

In Fig. 2 the dependence of the eigenvalues (EVs) on frequency ω for $\gamma=1$ is presented. Pure real EVs distributed all over the existence domain indicate the onset of an exponentially growing instability.

The growth rate of the instability is proportional to the absolute value of the corresponding pure real (or real part of the complex) EV. Weakly perturbed, low-amplitude plane waves (having large ω) become unstable during propagation

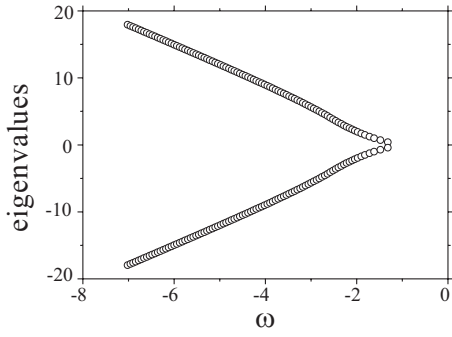


FIG. 2. Eigenvalue spectra of uniform solution for $\gamma=1$. Only the extremal values of pure real eigenvalues are shown.

and eventually split into a train of highly localized modes (see Fig. 3). The distance at which this filamentation occurs rapidly shortens with increase of the plane wave amplitude.

IV. SOLITARY SOLUTIONS

Although not integrable in the general case, our model equation possesses various steady-state solitary solutions, which are of fundamental interest for both energy transfer and light manipulation. From the realm of these solutions [25], here we are going to study only the two most fundamental bright symmetric unstaggered modes: on-site modes (having their maxima in one channel) and intersite ones (with maxima between two adjacent channels). The first part of this section is dedicated to localized structures far away from the boundaries of the uniform 1D array, whereas in the second part solitary solutions, which reside in the vicinity of the lattice surfaces, are investigated.

A. Lattice solitons

The discrete distribution of symmetric ($U_n = F_n e^{-i\omega\xi}$, $F_n = F_{-n}$, $n \in [-N/2, N/2]$, $|F_{n_c}| \gg |F_{n_c \pm 1}| \gg \dots \gg |F_{n_c \pm N/2}|$) on-site (os) mode amplitudes can be obtained from Eq. (3) and reads

$$F_{os} \equiv F(n_c = 0) = \sqrt{\frac{\omega + 2 - \gamma}{\omega + 2}}, \quad F_m = \eta^m F_{os}, \quad (7)$$

where n_c denotes the central channel of the lattice, $m \in [1, N/2]$, and $\eta = (\omega + 2 - \gamma)^{-1}$. On the other hand, for the symmetric intersite (is) mode, one can get

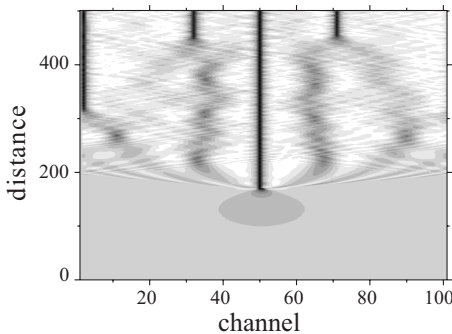


FIG. 3. Plane wave filamentation (top view) in a NWA consisting of 101 channels for $\omega=-1.06$. Black color corresponds to the intensity maximum.

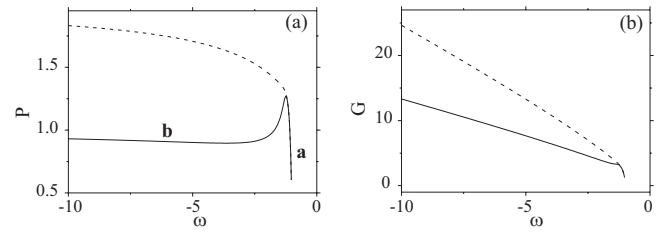


FIG. 4. (a) Dependence of power on propagation parameter ω for on-site unstaggered bright solitons (solid line) and intersite unstaggered bright solitons (dashed line). (b) Dependence of free energy G on propagation parameter ω for on-site (solid line) and intersite solitons (dashed line). The value of the nonlinearity parameter is in both cases fixed at $\gamma=1$.

$$F_{is} \equiv F(n_c = \pm 1) = \sqrt{\frac{\omega + 1 - \gamma}{\omega + 1}}, \quad F_{\pm m} = \eta^{m-1} F_{is}, \quad (8)$$

where η is defined as before while $m \in [1, N/2]$. Hereafter we focus on the stability and mobility issues of intensity-resonant lattice solitons while their interactions will be investigated elsewhere.

1. Stability consideration

Different methods to investigate soliton stability are discussed in the literature. For example, one can apply the energy principle [26] or deduce stability properties from Hamiltonian versus energy diagrams [27]. Here we use the linear stability analysis [28], in which fundamental soliton solutions are slightly perturbed $U_n = (F_n + \delta U_n e^{i\kappa n}) e^{-i\omega\xi}$, where $\delta U_n = a_n + ib_n$ is complex and $a_n, b_n \propto e^{\lambda\xi}$. The straightforward linearization procedure leads to the following eigenvalue problem:

$$\lambda \begin{pmatrix} a_n \\ b_n \end{pmatrix} = \begin{bmatrix} 0 & H^+ \\ -H^- & 0 \end{bmatrix} \begin{pmatrix} a_n \\ b_n \end{pmatrix} \equiv \mathbf{M} \begin{pmatrix} a_n \\ b_n \end{pmatrix}, \quad (9)$$

where the matrix \mathbf{M} (of size $2N \times 2N$ for the lattice with N sites) is, generally, non-Hermitian. The elements of the submatrices H^\pm are

$$H_{jk}^+ = \left(-(\omega - 2) - \frac{\gamma}{1 - u_j^2} \right) \delta_{jk} - \cos \kappa (\delta_{j,k+1} + \delta_{j,k-1}),$$

$$H_{jk}^- = H_{jk}^+ - \gamma \frac{u_j^2}{(1 - u_j^2)^2} \delta_{jk}. \quad (10)$$

According to Ref. [29], bright solitons are stable only if both the slope (i.e., Vakhitov-Kokolov) and spectral criteria are satisfied. The slope criterion [30] gives only a sufficient condition for soliton stability. Briefly, $dP/d\omega > 0$ and $dP/d\omega < 0$ correspond to unstable and (possibly) stable fundamental solitons. Figure 4(a) shows the power P as a function of propagation parameter ω and fixed $\gamma=1$ for both unstaggered on-site and intersite solitons. The power of solitons of the latter type is always higher than the power of on-site solitons for the same propagation constant. From this figure we can deduce that, at $\omega < -1.1$, two different fundamental on-site solitons can be found for a given power value. Both

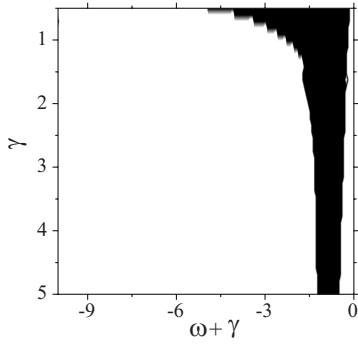


FIG. 5. Stability diagram of on-site bright solitons vs parameters γ and $\omega + \gamma$. The black area separating two stability areas corresponds to exponentially unstable on-site configurations.

solutions may be stable in the areas of branch *a* for $-1.2 < \omega < -1.1$ and branch *b* for $\omega < -4$, respectively. While solitons in branch *b* are strongly localized modes featuring a nearly single-site shape, solitons found in branch *a* extend over many lattice sites. These two regions with negative slope are separated by a narrow area with high power in which the slope condition is violated ($dP/d\omega > 0$ for fixed γ). For intersite solitons, the function $P(\omega)$ is monotonically decreasing with increasing parameter ω and fixed γ . However, being strictly adopted for fundamental one-site centered solitons, the application of the slope condition in the case of intersite structures is not appropriate.

Now we turn to the spectral condition. The corresponding stability results for on-site solitons are summarized in the diagram shown in Fig. 5. The unstable EVs for all on-site solitons located inside the black area in Fig. 5 are purely real: one positive real EV for $-2 < \omega < -1$ and two positive real EVs for $-3.5 < \omega < -2$. Therefore, the spectral condition for stability is violated. However, the spectral stability of the on-site solitons, declared by the purely imaginary EV spectrum, corresponds to the predictions of the slope criterion for both possibly stable on-site branches. In conclusion, it can be stated that on-site solitons for $-3.5 < \omega < -1$ are unstable. On the other hand, intersite solitons are exponentially unstable for the whole observed parameter space: one positive purely real EV in the EV spectrum is observed for all values of the parameter ω , thus violating the spectral condition for stability [29].

Knowing that there are unstable regions in the parameter space, it is interesting to reveal in what way instabilities develop. The on-site solitons are unstable in a narrow region of parameter space violating both the slope and spectral conditions. Being highly localized and with high power, they stay permanently localized and develop instability by gradually increasing their amplitude in an oscillatory manner, followed by radiation. The final state is a highly localized breather structure whose average amplitude corresponds to the amplitude of the closest stable on-site configuration; see Fig. 6(a). However, a slight transverse perturbation causes the unstable on-site solitons to diffract, as shown in Fig. 6(b).

The instability region of the intersite solitons can be associated with a violation of the spectral condition. As a consequence, the so-called drift instability introduced in [29] seems to be the way the intersite solitons develop instability

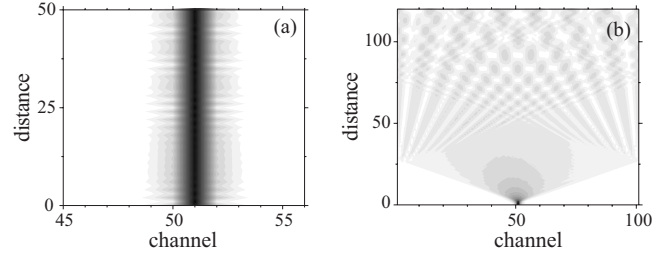


FIG. 6. (a) Slightly perturbed on-site soliton, belonging to the instability area in Figs. 4(a) and 5, with $\omega = -1.5$, $P = 1.083$, and $\gamma = 1$. The mode stays highly localized but changes its amplitude in an oscillatory manner—a breather is formed. (b) Diffraction of the on-site soliton in the presence of a small transverse perturbation.

in the range of small and moderate powers, i.e., in the range where the inter- and on-site solitons with the same power coexist, and in the range where inter- and on-site modes start to separate [Fig. 4(a)], respectively. In other words, a small perturbation will change an unstable mode to a breather solution localized around the neighboring lattice site. This transition is followed by more or less effective radiation, which depends on the type of perturbation (symmetric or asymmetric, amplitude of perturbation) and on both the slope and width of the perturbed mode. On the other hand, in the region of high-power intersite modes, $P \approx 2$, where an on-site soliton with the same power does not exist, intersite solitons are highly unstable under a symmetric perturbation, thus preventing numerics to give some definite answer on the fate of the final localized mode.

Here it is interesting to compare our discrete intensity-resonant model with the recently studied discrete nonpolynomial model [31], both of which have a singularity in the nonlinear term. In spite of a similar $P(\omega)$ dependence (Fig. 5(a), $\omega \equiv \mu$ in Ref. [31]), in a lattice possessing a nonpolynomial nonlinearity the slope of the $P(\omega)$ curve changes from positive to negative at a critical value of the propagation parameter for the on-site configuration. Therefore, in this model a narrow on-site soliton (branch *b* in Fig. 5(a), Ref. [31]) is unstable while its wider companion with the same power (branch *a* in Fig. 5(a), Ref. [31]) is stable, which is confirmed by the EV spectrum analysis. Finally, the intersite solitons, which are unstable in both cases in the whole parameter space, undergo amplitude and drift instability in the nonpolynomial and intensity-resonant cases, respectively.

2. Mobility consideration

In addition to being the simplest stationary solutions, these fundamental modes have a very important role in the concept of the Peierls-Nabarro (PN) barrier [25,32–34]. That is, discrete soliton motion across the lattice may be viewed as successive transformations from on-site to intersite modes with either Hamiltonian or free energy differences between modes, i.e., a discreteness-induced barrier that has to be overcome in order to move solitons sideways. Mobile solitons are found only in those regions in which the PN barrier vanishes (or is rather small). Although the PN concept is intuitively clear, its definition is not unique [32,35]. Here the

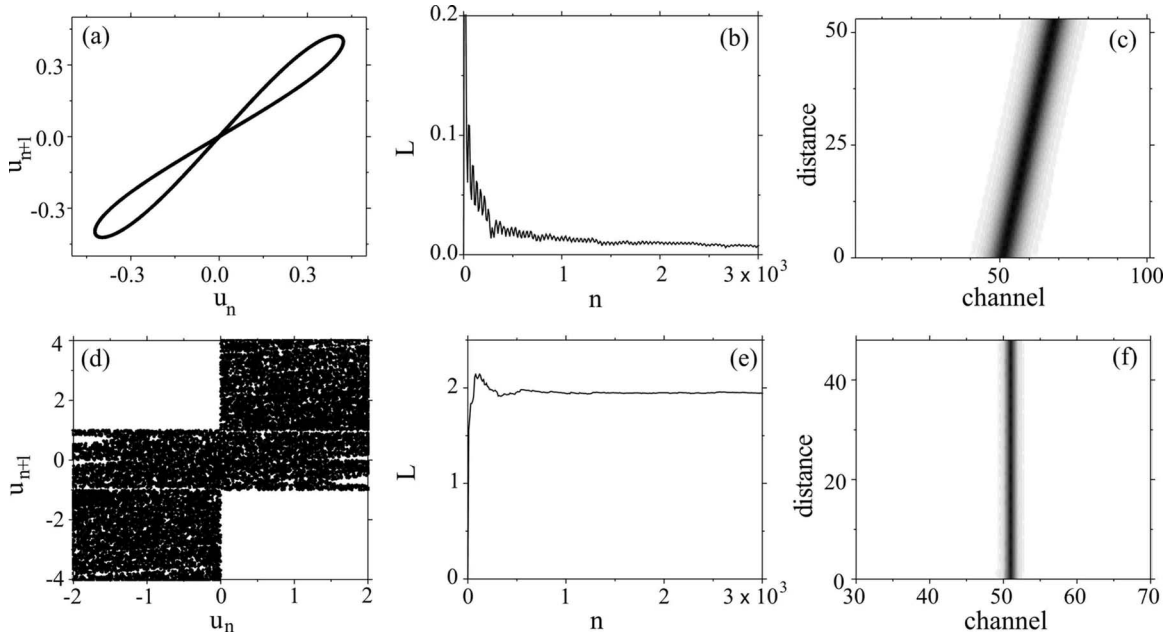


FIG. 7. Mappings (a) and (d) and corresponding Lyapunov exponents (b) and (e) for stable on-site solitons belonging to branch a ($P = 1.054$, $\omega = -1.1$) and to branch b ($P = 0.9017$, $\omega = -5$), respectively. Only in the first case can persistently moving localized structures be found. (c) Persistent motion of localized modes initiated by kicking the on-site soliton with $P = 1.054$, $\omega = -1.1$ which belongs to branch a , and (f) trapping of the soliton from branch b with $P = 0.902$, $\omega = -5$.

PN barrier for unstaggered solitons is discussed in the framework of free energy [36] and mapping analysis [35,37].

The PN barrier can be interpreted as the difference between the values of the free energy G for on-site and intersite stationary localized modes with equal values of the norm P , or equal values of ω [28,36],

$$(\Delta G_{\text{PN}})_P = (G_{\text{os}} - G_{\text{is}})_P = (\Delta H - P\Delta\mu)_P \quad (11)$$

or

$$(\Delta G_{\text{PN}})_\omega = (G_{\text{os}} - G_{\text{is}})_\omega = (\Delta H - \omega\Delta P)_\omega, \quad (12)$$

where $\Delta H = H_{\text{os}} - H_{\text{is}}$, $\Delta\omega = \omega_{\text{os}} - \omega_{\text{is}}$, and $\Delta P = P_{\text{os}} - P_{\text{is}}$. Here the second interpretation is taken into consideration because of the large separation of powers for on-site and intersite unstaggered configurations [see Fig. 5(b)].

In the present model, as in the situation in media with cubic nonlinearity [25,32], a vanishing PN barrier is observed only in a limited region of parameter space (ω, γ) where on-site (a branch) and intersite solitons with equal propagation constants and power have similar free energies, as can be seen in Fig. 4(b). Accordingly, mobile discrete solitons may originate only from the on-site branch a , and the corresponding intersite modes from this area. This is confirmed numerically by applying a transverse “kick” of size $\phi = \pi/18$; see Fig. 7(c).

The mapping analysis is based on the relation between the map that corresponds to the observed intensity-resonant model and a total integrable map corresponding to the discrete Ablowitz-Ladik (AL) equation [38]. In this approach, the intensity-resonant map, which is nonintegrable, is considered as a slight perturbation of the AL map. In Refs. [35,37] it was shown that dynamically *stable* localized structures

correlate with the emergence of chaotic areas in the corresponding map. Strictly, the first appearance of a localized structure is related to the existence of more or less perfect separatrices with merging stable and unstable manifolds of the saddle fixed point at the corresponding map origin [35,37]. While in the integrable and nearly integrable cases the separatrices are almost perfect, in nonintegrable systems the separatrix is not perfect, in the sense that stable and unstable manifolds intersect transversely at homoclinic points, giving rise to chaotic dynamics.

Following the developed procedure, the map corresponding to the stationary equation can be written as

$$u_{n+1} = (2 - \omega)u_n - \gamma \frac{u_n}{1 - u_n^2} - v_n, \quad v_{n+1} = u_n. \quad (13)$$

It can be found that this map possesses five fixed points, one of which is located at the origin, $u_n = v_n = 0$. The presence of a homoclinic orbit originating from the origin implies the existence of a bright fundamental soliton. Two examples are plotted in Figs. 7(a) and 7(d). The corresponding positive 1D Lyapunov exponents [37] [see Figs. 7(b) and 7(e)] are taken as a measure of the developed chaos, which is closely related to the existence of moving localized modes. From the viewpoint of the moving localized modes, the existence of a perfect, or nearly perfect, map separatrix indicates the vanishing of the PN barrier [35,37]. A change from the perfect map separatrix to an imperfect one with variation of a parameter is then interpreted as the emergence of the PN barrier. A perfect (or nearly perfect) map separatrix is a characteristic of the parameter space area where the on-site and intersite localized configurations with similar power coexist. Only in such cases can stable freely moving localized states be

generated by the application of a transverse kick to any of the mentioned localized configurations [see Figs. 7(c) and 7(f)].

B. Surface solitons

Surface solitons are strongly localized structures which may exist at the interface between two different media. Tamm incorporated previously neglected edge effects in a semi-infinite Kronig-Penney model and discovered that such strongly localized surface states can appear, provided that the surface potential perturbation is strong enough [39].

Recently it has been suggested that surface solitons may exist at the interface between a homogenous medium (substrate) and a NWA [40], followed soon afterward by the first experimental observation of discrete surface solitons in an AlGaAs NWA exhibiting a cubic self-focusing nonlinearity [41]. These first results triggered intensive investigations of nonlinear waves at surfaces and boundaries of NWAs. The existence of surface gap solitons in a lattice with cubic self-defocusing nonlinearity has been reported in Ref. [42]. Very recently, strongly localized surface waves were independently observed in NWAs exhibiting saturable [43,44] and quadratic nonlinearities [45], respectively.

As in uniform 1D lattices with cubic and saturable nonlinearities, we find a power threshold for formation of stable surface solitons [40,43]; see Fig. 8(a). Below the threshold $P \approx 0.56$ it is possible to observe a deflection of the launched beam from the interface. Some of the deflected beams can be trapped in channels close to the interface, while others may exhibit surface oscillations [46,47]. Linear stability analysis also indicates the existence of a marginally stable domain: the eigenvalues as a function of soliton frequency ω are given for $\gamma=3$ in Fig. 8(b). An example of an on-site surface soliton with $\omega=-4.84$ and its stable propagation along the array are shown in Figs. 8(c) and 8(d), respectively. On the other hand, intensity-resonant intersite surface solitons formed above the threshold are shown to be always unstable and they usually quickly transform into the more stable on-site configurations.

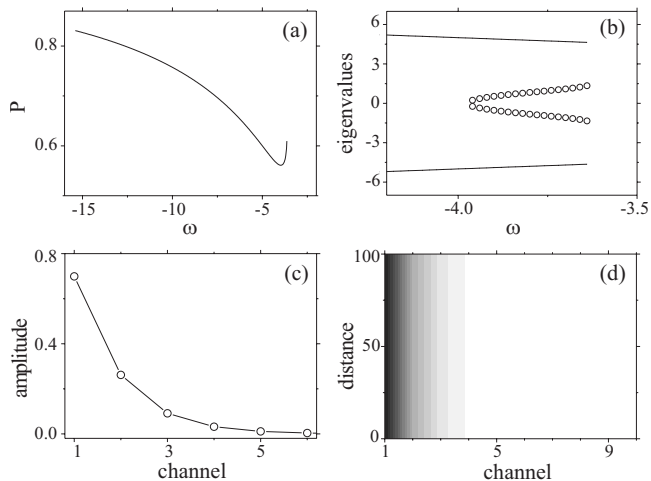


FIG. 8. (a) Soliton power versus soliton frequency for $\gamma=3$. (b) The eigenvalue spectrum for on-site solitons (pure real eigenvalues, circles; extremal pure imaginary eigenvalues, solid lines). (c) Form of symmetric on-site surface soliton for $\omega=-4.84$ and (d) stable propagation of this soliton.

V. CONCLUSIONS

In conclusion, we propose a theoretical model to describe beam propagation in periodic, one-dimensional media with intensity-resonant nonlinearity. We find the corresponding band structure and integral of motions and recognize the regions in the parameter space in which modulational instability may occur. Approximate expressions for the two most fundamental types of bright lattice solitons are given. Both stability and mobility issues of these strongly localized structures have been investigated. The dynamical behavior of modes localized at the lattice-substrate interface has been studied, too. All results are supported numerically.

ACKNOWLEDGMENT

This work has been supported by the Ministry of Science of Republic Serbia (Project No. 141034).

- [1] A. Trombettoni and A. Smerzi, *Phys. Rev. Lett.* **86**, 2353 (2001).
- [2] S. F. Mingaleev, P. L. Christiansen, Y. B. Gaididei, M. Johansson, and K. Ø. Rasmussen, *J. Biol. Phys.* **25**, 41 (1999).
- [3] M. Sato, S. Yasui, M. Kimura, T. Hikihara, and A. J. Sievers, *Europhys. Lett.* **80**, 30002 (2007).
- [4] D. N. Christodoulides and R. I. Joseph, *Opt. Lett.* **13**, 794 (1988).
- [5] H. S. Eisenberg, Y. Silberberg, R. Morandotti, A. R. Boyd, and J. S. Aitchison, *Phys. Rev. Lett.* **81**, 3383 (1998).
- [6] R. Iwanow, R. Schiek, G. I. Stegeman, T. Pertsch, F. Lederer, Y. Min, and W. Sohler, *Phys. Rev. Lett.* **93**, 113902 (2004).
- [7] J. W. Fleischer, T. Carmon, M. Segev, N. K. Efremidis, and D. N. Christodoulides, *Phys. Rev. Lett.* **90**, 023902 (2003).
- [8] A. Fratallocchi, G. Assanto, K. A. Brzdakiewicz, and M. A. Karpierz, *Opt. Lett.* **29**, 1530 (2004).
- [9] G. I. Stegeman and T. E. Torruellas, *Philos. Trans. R. Soc. London, Ser. A* **354**, 745 (1996).
- [10] B. Mainguet, *Opt. Lett.* **13**, 657 (1988).
- [11] G. Picoli, P. Gravey, C. Ozkul, and V. Vieux, *J. Appl. Phys.* **66**, 3798 (1989).
- [12] M. Chauvet, S. A. Hawkins, G. J. Salamo, M. Segev, D. F. Bliss, and G. Bryant, *Opt. Lett.* **21**, 1333 (1996).
- [13] R. Uzdin, M. Segev, and G. J. Salamo, *Opt. Lett.* **26**, 1547 (2001).
- [14] N. Fressengeas, N. Khelifaoui, C. Dan, D. Wolfersberger, G. Montemezzani, H. Leblond, and M. Chauvet, *Phys. Rev. A* **75**, 063834 (2007).
- [15] D. Wolfersberger, N. Khelifaoui, C. Dan, N. Fressengeas, and H. Leblond, *Appl. Phys. Lett.* **92**, 021106 (2008).

- [16] F. Chen, M. Stepić, C. E. Rüter, D. Runde, V. Shandarov, D. Kip, O. Manela, and M. Segev, *Opt. Express* **13**, 4314 (2005).
- [17] K. Inoue and K. Ohtaka, *Photonic Crystals: Physics, Fabrication and Applications*, Springer Series in Optical Sciences Vol. 94 (Springer, Berlin, 2004).
- [18] D. N. Christodoulides and M. I. Carvalho, *J. Opt. Soc. Am. B* **12**, 1628 (1995).
- [19] D. Mandelik, H. S. Eisenberg, Y. Silberberg, R. Morandotti, and J. S. Aitchison, *Phys. Rev. Lett.* **90**, 053902 (2003).
- [20] W. Chen and D. L. Mills, *Phys. Rev. Lett.* **58**, 160 (1987).
- [21] M. Stepić, D. Kip, Lj. Hadžievski, and A. Maluckov, *Phys. Rev. E* **69**, 066618 (2004).
- [22] J. Meier, G. I. Stegeman, D. N. Christodoulides, Y. Silberberg, R. Morandotti, H. Yang, G. Salamo, M. Sorel, and J. S. Aitchison, *Phys. Rev. Lett.* **92**, 163902 (2004).
- [23] Yu. S. Kivshar, *Opt. Lett.* **18**, 1147 (1993).
- [24] M. Stepić, C. Wirth, C. E. Rüter, and D. Kip, *Opt. Lett.* **31**, 247 (2006).
- [25] F. Lederer, G. I. Stegeman, D. N. Christodoulides, G. Assanto, M. Segev, and Y. Silberberg, *Phys. Rep.* **463**, 1 (2008).
- [26] E. W. Laedke and K. H. Spatschek, *Phys. Rev. Lett.* **41**, 1798 (1978).
- [27] N. Akhmediev, A. Ankiewicz, and R. Grimshaw, *Phys. Rev. E* **59**, 6088 (1999).
- [28] A. Maluckov, Lj. Hadžievski, and B. A. Malomed, *Phys. Rev. E* **76**, 046605 (2007).
- [29] Y. Sivan, G. Fibich, B. Ilan, and M. I. Weinstein, *Phys. Rev. E* **78**, 046602 (2008).
- [30] M. G. Vakhitov and A. A. Kolokolov, *Izv. Vyssh. Uchebn. Zaved., Radiofiz.* **16**, 1020 (1973) [*Radiophys. Quantum Electron.* **16**, 783 (1973)].
- [31] A. Maluckov, Lj. Hadžievski, B. A. Malomed, and L. Salasnich, *Phys. Rev. A* **78**, 013616 (2008).
- [32] Yu. S. Kivshar and D. K. Campbell, *Phys. Rev. E* **48**, 3077 (1993).
- [33] Lj. Hadžievski, A. Maluckov, M. Stepić, and D. Kip, *Phys. Rev. Lett.* **93**, 033901 (2004).
- [34] H. Susanto, P. G. Kevrekidis, R. Carretero-Gonzalez, B. A. Malomed, and D. J. Frantzeskakis, *Phys. Rev. Lett.* **99**, 214103 (2007).
- [35] S. Aubry, *Physica D* **7**, 240 (1983).
- [36] T. R. O. Melvin, A. R. Champneys, P. G. Kevrekidis, and J. Cuevas, *Phys. Rev. Lett.* **97**, 124101 (2006).
- [37] A. Maluckov, Lj. Hadžievski, and M. Stepić, *Physica D* **216**, 95 (2006).
- [38] D. Hennig and G. P. Tsironis, *Phys. Rep.* **307**, 333 (1999).
- [39] I. Tamm, *Phys. Z. Sowjetunion* **1**, 733 (1932).
- [40] K. G. Makris, S. Suntssov, D. N. Christodoulides, G. I. Stegeman, and A. Haché, *Opt. Lett.* **30**, 2466 (2005).
- [41] S. Suntssov, K. G. Makris, D. N. Christodoulides, G. I. Stegeman, A. Haché, R. Morandotti, H. Yang, G. Salamo, and M. Sorel, *Phys. Rev. Lett.* **96**, 063901 (2006).
- [42] Y. V. Kartashov, L. Torner, and V. A. Vysloukh, *Phys. Rev. Lett.* **96**, 073901 (2006).
- [43] E. Smirnov, M. Stepić, C. E. Rüter, D. Kip, and V. Shandarov, *Opt. Lett.* **31**, 2338 (2006).
- [44] C. R. Rosberg, D. N. Neshev, W. Krolikowski, A. Mitchell, R. A. Vicencio, M. I. Molina, and Yu. S. Kivshar, *Phys. Rev. Lett.* **97**, 083901 (2006).
- [45] G. A. Siviloglou, K. G. Makris, R. Iwanow, R. Schiek, D. N. Christodoulides, G. I. Stegeman, Y. Min, and W. Sohler, *Opt. Express* **14**, 5508 (2006).
- [46] M. Stepić, E. Smirnov, C. E. Rüter, D. Kip, A. Maluckov, and Lj. Hadžievski, *Opt. Lett.* **32**, 823 (2006).
- [47] S. Longhi, *Phys. Rev. A* **77**, 035802 (2008).